Noname manuscript No.
(will be inserted by the editor)

Modal Analysis of Monolithic and Jointed type Cantilever Beams with Non-Uniform Section

Bimal Purohit · Prakash Chand Jain · Ashok Kumar Pandey

Received: July 2015 / Accepted: February 2016

This is the accepted form of the Authors' copy. The final publication is available at Springer via http://dx.doi.org/10.1007/s11340-016-0149-y

Abstract Modal analysis of non-uniform bolted structures are of significance in modeling many complex mechanical structures. There are vast literatures available related with the analytical as well as numerical modeling of bolted joint. However, most of the analytical model discuss about the modeling of first mode of uniform structures with single bolted joint. In this paper, we present the modeling of single as well as bolted non-uniform beams using approximate mode shapes. To develop the model, we first carry out experiments to measures the modal frequencies and shapes of the test structures. Subsequently, we also do numerical modeling of non-uniform beams in ANSYS to verify the validity of the Euler-Bernoulli beam

Bimal Purohit
Vehicle Dynamics Lab, Mechanical and Aerospace Engineering
Indian Institute of Technology Hyerabad India

Prakash Chand Jain
Flight Structures Division
Defence Research and Development Laboratory, Hyderabad, India

Ashok Kumar Pandey
Vehicle Dynamics Lab, Mechanical and Aerospace Engineering
Indian Institute of Technology Hyderabad, Kandi, India Tel.: +91-40-23016085
Fax: +91-40-23016032
E-mail: ashok@iith.ac.in

theory in developing the analytical models. Finally, using the Euler-Bernoulli beam theory, we obtain the analytical values of frequencies using the approximate the mode shapes. The analytical results are found to be closer to the experimental results with a maximum percentage error of about 15%. The model presented in the paper can be extended to the mechanical structures with many non-uniform sections with or without bolted joints.

Keywords Non-uniform beam · Bolted structures · Model analysis · Closed form solution

1 Introduction

Majority of mechanical and aerospace structures are frequently modeled as non-uniform free-free Euler-Bernoulli beam [1–4]. Although, there have been many work on the modal analysis of a structure with varying mass but there are limited studies available for a system of structures with varying cross sections which are connected by bolted joints. Since jointed type cylindrical structures find application in rockets and space crafts, as sections of smaller lengths are joined together to form the full lengths, the analysis of non-uniform beams connected by bolted joint is very significant from various practical considerations. In this paper, we deal with the modal analysis of single as well as bolted cantilever beams with non-uniform sections.

Abrate [5] studied the vibration of non-uniform rods for which he transformed the equation of motions into the wave equation and found out that the natural frequencies of non uniform rods fixed at both ends is same as that of uniform rods. Wu and Ho [6] obtained the natural frequencies and mode shapes corresponding to the longitudinal and torsional vibrations of a non-uniform ship hull with large hatch openings using the finite-element method. Platus [2] employed Lagrangian approach to study nonlinear aeroelastic stability of flexible structure having non-uniform sections. Pourtakdoust and Assadian [7] studied the effect of thurst on the bending behaviour of non-uniform flexible floating structure. Jaworski and Dowell

[8] obtained the theoretical and experimental frequencies of a cantilever beam with multiple steps using the Rayleigh-Ritz method. Zheng et al. [9] developed modified vibration functions by satisfying the required boundary conditions to compute the frequencies of a multi-span beams with non-uniform sections subjected to moving loads. However, none of the above studies assumed the joints as bolted joint. To model the jointed structure, there exist different types of models which are classified based on loading, damping, flexibility of the joints, etc [10]. While the normally loaded joint produces less damping as compared to tangentially loaded joint, the damping in tangentially loaded joint depends on its elastic and plastic deformation due to micro- and macro-slip phenomena. Such behavior can be modeled using finely meshed finite element models or different friction models. Some of friction models are the Coulomb models, Masing model, Iwan model, etc. The nonlinear hysteretic behavior can be capture by different arrangements of Jenkin element, which is a combination of spring and friction slider, or the Bouc Wen model, etc. More details about the joint modeling can be found in reference [10, 11]. Oldfield et al. [12] used simplified models of bolted joints as a combination of the number of Jenkins elements and the Bouc-Wen model to study the effect of harmonic loading on a bolted joint using finite element method. Todd et al. [13] performed experiments on a beam with its boundaries supported by spring modified fasteners. Subsequently, they modeled the bolted joint with an effective spring stiffness based on the perpendicular load acting normal to the axis of the joint, i.e., neglecting the shearing effect, and thus, the effect of friction. Ouyang et al [14] conducted experiment on a single joint of two beams under torsional dynamic loads and described the hysteresis phenomena under different preloads and excitation amplitudes. Finally, they correlated the results with the micro and macro-slip phenomena at the joint interface. Ma et al [15] performed experiment on the bolted and unbolted structure. They found the nonlinear stiffness and damping associated the bolted joint by comparing the numerical model with the unbolted joint. Hartwigsen et al [16] performed experiment to characterize the

non-linear effect of a shear lap joint on the dynamics of two mechanical structure. They modeled the effective stiffness and damping effect using Iwan models. Quinn [17] presented the modal analysis of jointed structures by modeling the elastic effect of the joint using a linear modal equation and the dissipative effect of the joint with a continuum series-series Iwan model. Tol and Özgüven [18] described an experimental identification method based on frequency response function decouling and optimization to extract the joint properties in terms of translation, rotational, and cross-coupling stiffness and damping values. Chen et al. [19] used the numerical assembly method (NAM) for computing the natural frequencies of a cantilever beam having multiple spans of different cross-sections carrying spring-mass system at different locations. In this method, they considered the joints as attaching points of two beams, and, then, used the equilibrium and compatibility equations to form element matrices to compute the natural frequencies. Song et al [20] presented the modeling of bolted beam structure using finite element method with adjusted Iwan beam elements obtained by taking two adjusted Iwan model corresponding to each degrees of freedom of 2-noded beam element. Subsequently, they used multi-layer feed forward neural network to optimize the joint parameters obtained from FEM model with the measured results. Eriten et al [21] ultilized nonlinear system identification and reduced order modeling to extract the nonlinear damping of beams with bolted joints. They have also compared the results with monolithic structure. Ahmadian and Jalali [22] presented a nonlinear parametric formulation through a generic element under the conditions of a joint interface. They obtained the dynamic characteristics of joint by comparing the dynamic response of generic element using the incremental harmonic balance with the observed behavior of the structure. To do accurate nonlinear friction modeling of the jointed structure for general structure, Süß and Willner [23] first used three degree-of-freedom model using multiharmonic balance method (MHBM) and then extended it to n degrees-of-freedom model using the finite element method. Since the accuracy of harmonic balance method increases with the number of har-

monics, increase in harmonics leads to larger computation time. To reduce the computation time, Jaumouillé et al [24] proposed an adjusted harmonic balance method which adjusts the number of retained harmonics for a given precision and frequency value. Although there have been many improvement in the modeling of bolted structures, however, some level of uncertainties remains due to non-smooth nonlinear dynamic characteristics [25]. It is also important to note that most of the above literatures dealt with the bolted joint of only uniform beams. To do the modeling of jointed beams with non-uniform beams, Sarkar and Ganguli, [26], adopted an inverse problem approach to obtain fundamental mode shape of a single as well as bolted non-uniform Euler Bernoulli beams by approximating the variation of mass and flexural rigidity by polynomial of required order in conjunction with free-free Euler-Bernoulli beam. To do the analysis of bolted non-uniform beam, they modeled the bolted joint with torsional spring. However, their analysis was limited to the first mode of simply-supported non-uniform beam. In this paper, we focus on the modal analysis of jointed cantilever beams with two and three non-uniform sections using higher modes.

To do the analysis, we first perform the experiments to measure the mode shapes and frequencies of bolted cantilever beams. Based on the measured locations of the zero positions of first, second and third mode shapes, we compute approximate modeshapes of non-uniform cantilevers with bolted joints based on the same approach as suggested by Sarkar and Ganguli [26]. Finally, we compute the frequencies of first three transverse modes of bolted cantilever with non-uniform sections and compare with the experiments.

2 Expermental Procedure and Results

To measure the modal frequencies of single as well as bolted non-uniform beams as shown in Fig. 1(b), we use Polytec scanning laser vibrometer as described in Fig. 1(a). To perform the experiment, we first mount the test specimen on a shaker. Subsequently, we apply pseudorandom signal from an internal function generator

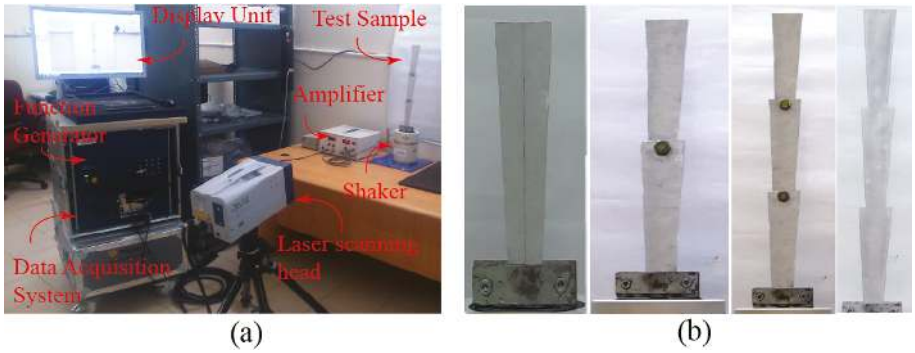

Fig. 1 (a) A picture showing the outline of experimental setup; (b) Test specimen showing the images of single non-uniform beam, bolted beams with two and three non-uniform sections, and a monolithic beam with three non-uniform sections without bolted joint.

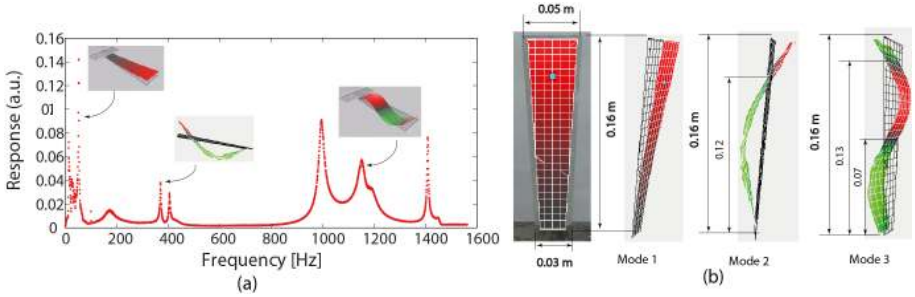

Fig. 2 (a) Experimental frequency response of a single non-uniform beam with diverging section from the fixed end. (b) The scanning points and zero locations are shown in its first, second and the third modes, respectively.

of vibrometer over a frequency bandwidth of around 200 Hz to 1600 Hz so as to cover the first three transverse modes of different configurations. In each case, the FFT lines are taken as 3200 over the given bandwidth. The acceleration of shaker is controlled through the amplifier. To capture the mode shape and modal frequencies, we defined sufficient number of scanning points on the test sample using laser scanning head and start the measurements of displacement/velocity at each points of the defined region. The movement of laser over the scan points are controlled using OFV controller. Finally, the measured quantities such as the displacement or velocity and input signal are stored using data acquisition system over a given frequency range. The accuracy of frequency measurements depends on the number of FFT lines and frequency bandwidth. An accuracy of corresponding mode

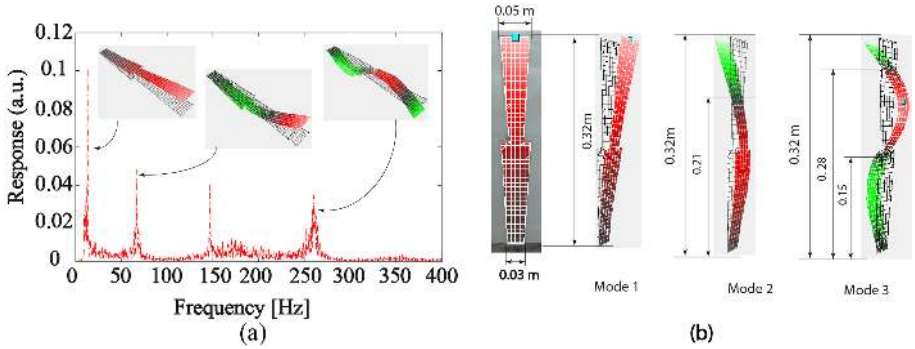

Fig. 3 (a) Experimental frequency response of a bolted beam with two sections. (b) The scanning points and the zero locations are shown in its first, second and the third modes, respectively.

shapes depends on the sufficient number of scan points. A detailed description of measurement technique is described in the references [15, 27, 28].

Using the above mentioned procedure, we perform experiments to find the modal frequencies and mode shapes of single as well as bolted non-uniform beams as shown in Fig. 1. All the beams are made of aluminium and are of length, $L = 0.16$ m, thickness, $t = 0.002$m and have varying width of $b_1 = 0.03$ m at one end to $b_2 = 0.05$ m at another end. Each beam is provided with end holes of diameter $d = 0.01$ m and an extra length of 0.02 m was provided for the fastening. The Young's modulus and the density of aluminium beam are taken as $E = 69$ GPa and $\rho = 2700$ kg/m^3. To increase the accuracy of mode shape, we divide the beam length into 22-32 divisions. Similarly, the beam width with smaller side is divided into 4-6 divisions and that with larger side is divided into 6-8 divisions. Consequently, for the beam of length 0.16 m, approximate spacing between each scanning points along the beam length vary from 0.005 m to 0.007 m.

Table 1 Experimental results for single and bolted non-uniform cantilever beams.

Beam configurations	1^{st} mode [Hz]	2^{nd} mode [Hz]	3^{rd} mode [Hz]
Single beam(Small end fixed)	54.68	371.09	1146.48
Two section bolted beam	13.1	66.5	260.25
Three sections bolted beam	5.62	33.43	73.44
Three sections monolithic beam	6.75	43.50	118.0

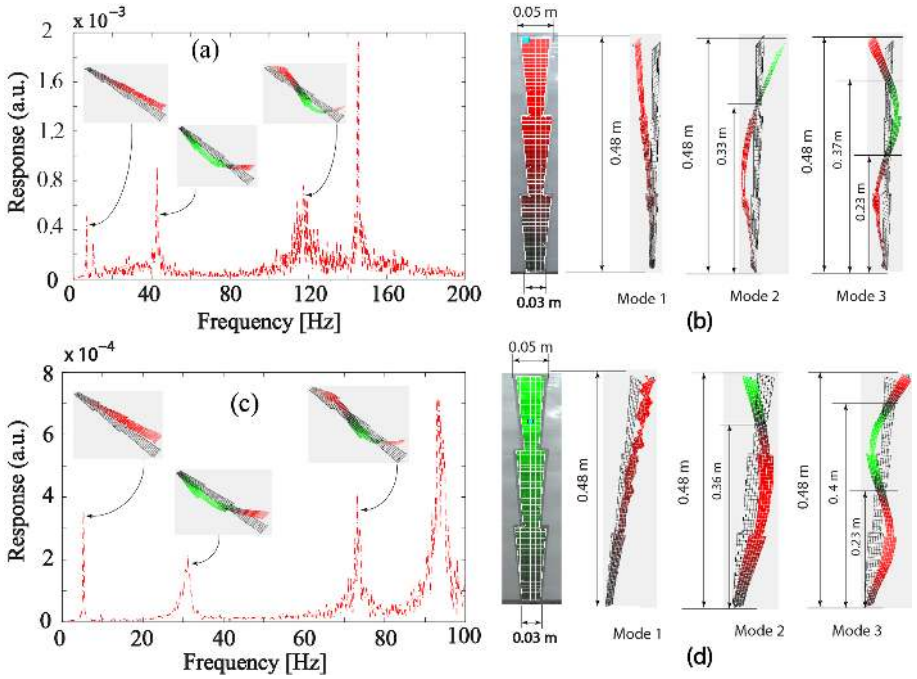

Fig. 4 (a) Experimental frequency response of a bolted beam with three non-uniform sections; (b) The scanning points and the zero locations of the bolted beams are also shown in its first, second and the third modes, respectively. (c) Experimental frequency response of a monolithic beam with three non-uniform sections without joint; (d) The scanning points and the zero locations of the monolithic beams are also shown in its first, second and the third modes, respectively.

To systematically perform the experimental studies, we first perform experiments on a single non-uniform cantilever beam. Figure 2(a) shows the frequency response of the single non-uniform cantilever beam when the smaller end is fixed as shown in Fig. 1(b). The measured frequencies are found as 66.40 Hz, 401.36 Hz, and 1160.15 Hz. Based on the observation of second mode, it is found that the first torsional and second transverse modes are closer to each other. Figure 2(b) shows the scanning points over the length and width of the beam. It also shows the zero locations along the length of the beam at $x = 0$ m for first mode, $x = 0$ and 0.12m for second mode, and $x = 0$, 0.07 and 0.13m for third modes, respectively. Although, the zero points for a given mode is found corresponding to the zero response amplitude, there may be some error if the zero point is located between the two scanning points. We performed measurements by varying

the scanning points along the length from 27 to 33. Therefore, the maximum error associated with the measurement of zero points may vary from 0.005m to 0.006m. Figure 3(a) shows the variation of frequency response of a bolted cantilever beam with two non-uniform sections. The frequencies are found to be 13.1 Hz 66.5 Hz, and 260.25 Hz corresponding to first three transverse modes of the beam. The corresponding zero points are found to be $x = 0$ m for first mode, $x = 0$ and 0.21m for second mode, and $x = 0$, 0.15 and 0.28m for third modes, respectively, as shown in Figure 3(b). Similarly, the number of scanning points over each section along the length is taken about 23 points which leads to a difference of about 0.007m between two neighboring points.

Figures 4(a) and (c) show the frequency response curves of cantilever beams with three non-uniform sections with and without bolted joints, respectively. For the cantilever beam with three non-uniform bolted sections are found at 5.625 Hz, 33.43 Hz, and 73.44 Hz, respectively. The zero points are found to be $x = 0$ m for first mode, $x = 0$ and 0.33m for second mode, and $x = 0$, 0.37 and 0.23m for third modes, respectively, as shown in Figure 4(b). For the cantilever beam of three non-uniform sections without any bolted joints, the transverse modes are found at 7.25 Hz, 42.75 Hz, and 120.75 Hz, respectively. The zero points are $x = 0$ m for first mode, $x = 0$ and 0.36m for second mode, and $x = 0$, 0.4 and 0.23m for third modes, respectively, as shown in Figure 4(d). In both the cases, for the scanning points of 23 per section in both the cases, the maxiumum difference between two points is about 0.007m. The comparison of results between monolithic and bolted section show that the beam with bolted joints has lower modal frequencies than that of the monolithic beam due to marginal reduction in stiffness and mass of the bolts at the joints. The measured frequencies in all the above cases are summerized in Table 1. In the subsequent section, we first present the modeling of single non-uniform beam and monolithic three sections beam using ANSYS. Subsequently, we present analytical modeling of a single non-uniform beam and the bolted beam using lumped spring at the joint. The error associated with the measured values

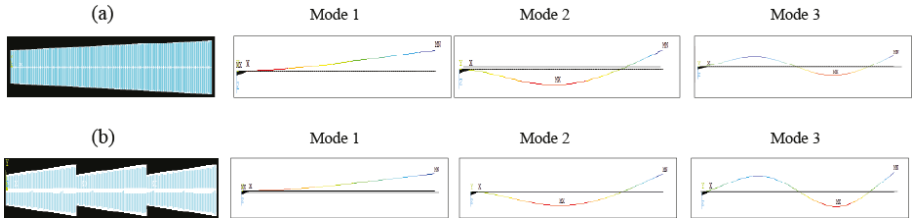

Fig. 5 Finite element models and mode shapes of (a)single beam with diverging section, (b) single beam with converging section, (c) a monolithic beam with three non-uniform sections without any joints.

may vary from 0.25 to 1 Hz due to the number of FFT lines taken for a given range of measured frequencies.

3 Numerical Modelling and Results

In this section, we present numerical modeling of single as well as monolithic non-uniform beams using 2D beam element in ANSYS. To model different sections, the cross-sections at $x = 0$ and $x = L$ are provided corresponding to the dimensions of single non-uniform beam. To model the beams of monolithic beam with three non-uniform sections, we provide six cross-sections corresponding to the ends of each section and glue them together. After providing the material properties of the beams, we perform modal analysis using block lancoz method to compute modal frequencies and corresponding modes of the single and bolted non-uniform beams. Figure 5(a) shows the numerically computed first three transverse mode shapes of non-uniform beam when smaller end is fixed. Similarly, we obtain the first three transverse modes of monolithic cantilever beam with three non-uniform sections as shown in Fig. 5(c). The frequency values of beams with single and three non-uniform sections are summerized in Table 2.

Table 2 Frequencies of cantilever beam with single and monolithic three non-uniform sections.

FEA models	1^{st} mode [Hz]	2^{nd} mode [Hz]	3^{rd} mode [Hz]
Single beam(Small end fixed)	54.49	380.75	1100
Three sections monolithic beam	6.64	41.88	118.43

On comparing the numerical results from Table 2 with the experimental results as mentioned in Table 1, we get very good agreement with a minimum and maximum percentage errors of 0.3% and 11%, respectively.

4 Analytical Procedure and Results

In this section, we present approximate method to compute the first three transverse mode shapes of the single non-uniform cantilever beam with variable mass and elastic rigidity by following the approach proposed by Sarkar and Ganguli [26]. Later, we utilize the computed mode shape to obtain the modal frequencies using Rayleigh-Ritz method. After validating the method with the results of the single beams, we compute the mode shapes and frequencies of bolted cantilever beams with two and three non-uniform sections, respectively. Finally, we compare the analytical results with experimental results for all the cases and discuss the results.

4.1 Modal Analysis of a Single Non-Uniform Beam

To compute the expression of mode shapes corresponding to first three transverse modes of a non-uniform cantilever beam fixed at its smaller end, we use zero positions from the measured mode shapes. Subsequently, we use the Rayleigh-Ritz method to compute the frequencies.

Taking the same dimensions as taken for the test sample for a beam of length $L = 0.16$m, width $b_1 = 0.03$ m at the small end and $b_2 = 0.05$ m at the larger end, thickness, $h = 0.002$ m, the elastic modulus of $E = 69$ GPa and the density of $\rho = 2700$ kg/m^3, the transverse motion can be governed by the Euler-Bernoulli beam equation as [26],

$$\frac{\partial^2}{\partial x^2}\left(EI(x)\frac{\partial^2 \phi}{\partial x^2}\right) - m(x)\omega^2\phi(x) = 0, \tag{1}$$

where, $\phi(x)$ is the unknown mode shape corresponding to the modal frequency ω which is obtained by satisfying the corresponding boundary conditions and the governing equation of the beam. Due to the variation of width along the length, the variation of mass $m(x)$ and the flexural rigidity $EI(x)$ can be obtained as

$$m(x) = 0.162 + 0.675x, \quad \text{and} \quad EI(x) = 1.38 + 5.75x. \tag{2}$$

After finding the approximate mode shape, we obtain the corresponding frequency using the Rayleigh-Ritz method as

$$\omega_n^2 = \frac{\sum_i \int_0^L \frac{\partial^2}{\partial x^2}\left(EI(x)_i \frac{\partial^2 \phi_{ni}(x)}{\partial x^2}\right)\phi_{ni}(x)dx}{\sum \int_0^L m(x)_i \phi_{ni}^2(x)dx} \tag{3}$$

where, ω_n is the angular frequency and $f_n = \frac{\omega_n}{2\pi}$ is the frequency in Hz, ϕ_{ni} is the mode shape of i^{th} section of the bolted beam corresponding to n^{th} mode and for the single beam, $i = 1$.

To describe the procedure of obtaining approximate mode shape a single non-uniform beam corresponding to n^{th} mode, we take $i = 1$.

– *First Mode*: For the first mode of the single non-uniform cantilever beam, we approximate the assumed mode shape ϕ_{11} by a polynomial expression

$$\phi_{11}(x) = c_0 + c_1\frac{x}{L} + c_2\left(\frac{x}{L}\right)^2 + c_3\left(\frac{x}{L}\right)^3 + c_4\left(\frac{x}{L}\right)^4, \tag{4}$$

where, c_0, c_1, c_2, c_3, c_4 are five unknown coefficients. These unknowns are determined using the boundary conditions and normalization condition as follow.

$$\phi_{11}(0) = 0,\ \phi'_{11}(0) = 0, \phi''_{11}(L) = 0, \phi'''_{11}(L) = 0, \phi_{11}(L) = 1, \tag{5}$$

On solving the above equation, we obtain the following form of the first mode

$$\phi_{11}(x) = 78.125x^2 - 325.52x^3 + 508.63x^4. \tag{6}$$

Using Eqs. (3) and (6), we get the frequency of first mode as 54.5 Hz.

– *Second Mode*: By observing the second mode shape of single beam with lower end fixed from the experimental and numerical simulation from Figs. 2 and 5, we noticed that there exist an additional zero position at $\alpha = 0.12$m from the fixed end. Consequently, the order of the assumed polynomial for the second mode shape is increased by one in order to satisfy additional zero position boundary condition. Therefore, the assumed mode shape can be written as

$$\phi_{21}(x) = c_0 + c_1\left(\frac{x}{L}\right) + c_2\left(\frac{x}{L}\right)^2 + c_3\left(\frac{x}{L}\right)^3 + c_4\left(\frac{x}{L}\right)^4 + c_5\left(\frac{x}{L}\right)^5. \quad (7)$$

The unknown coefficients $c_0, c_1, c_2, c_3, c_4, c_5$ can be obtained from the following conditions:

$$\phi_{21}(0) = 0,\ \phi'_{21}(0) = 0, \phi''_{21}(L) = 0, \phi'''_{21}(L) = 0, \phi_{21}(\alpha) = 0, \phi_{21}(L) = 1 \quad (8)$$

where, $\alpha = 0.12$ m is the zero-location of second mode. Solving the above equations, we obtain the final form of mode shape as

$$\phi_{21}(x) = -581.60x^2 + 9295.43x^3 - 46737.11x^4 + 80532.50x^5. \quad (9)$$

Using Eqs. (3) and (9), we get the frequency of first mode as 378.56 Hz. The errors associated with the measured values of zero location $\alpha = 0.12 \pm 0.006$m may vary from 2% when $\alpha = 0.126$m to 6% when $\alpha = 0.114$m. These errors can be reduced by increasing the number of scanning points on the beam.

– *Third Mode*: Like the case of second mode, by observing the modes of single beam from the experimental and numerical results as shown in Figs. 2 and 5, we noticed two additional zero locations at $\beta = 0.07$m and $\alpha = 0.13$ m from the fixed end. Consequently, the assumed mode shape can be approximated with the polynomial expression of order six, i.e., one order higher to the second

mode to satisfy the extra zero conditions. The mode shape is given by

$$\phi_{31}(x) = c_0 + c_1\left(\frac{x}{L}\right) + c_2\left(\frac{x}{L}\right)^2 + c_3\left(\frac{x}{L}\right)^3 + c_4\left(\frac{x}{L}\right)^4 + c_5\left(\frac{x}{L}\right)^5 + c_6\left(\frac{x}{L}\right)^6 \tag{10}$$

The unknown coefficients c_0, c_1, c_2, c_3, c_4, c_5 and c_6 can be obtained from the following conditions:

$$\phi_{31}(0) = 0,\ \phi'_{31}(0) = 0, \phi''_{31}(L) = 0, \phi'''_{31}(L) = 0, \phi_{31}(\beta) = 0, \phi_{31}(\alpha) = 0, \phi_{31}(L) = 1 \tag{11}$$

where, $\beta = 0.07$ m and $\alpha = 0.13$ m are zero positions. On solving Eq. (11), we get the following form of the mode shape

$$\phi_{31}(x) = 1422.53x^2 - 44591.89x^3 + 4.82 \times 10^5 x^4 - 2.19 \times 10^6 x^5 + 3.61 \times 10^6 x^6. \tag{12}$$

Using Eqs. (3) and (12), we get the frequency of third mode as 1007.87 Hz. Taking the possible variation of zero locations as $\beta = 0.07 \pm 0.006$m and $\alpha = 0.13 \pm 0.006$ m, the percentage error in computing the frequency may vary from 5.7% to 14.5%. Therefore, measurement of zero location is very important to compute the accurate frequency of non-uniform beams.

Table 3 Frequencies of single non-uniform beam with diverging section.

Modes	Exp. Result [Hz]	Anal. Result [Hz]	Num. Result [Hz]
1st mode	54.68	54.5	54.49
2nd mode	371.09	378.56	380.75
3rd mode	1146.48	1007.87	1100

On comparing the analytical solutions with the experimental and numerical results in Table 3, we found that the percentage error for the first mode is less than 1%, the second mode is about 2% and the third mode is about 12% with respect to the experimental results.

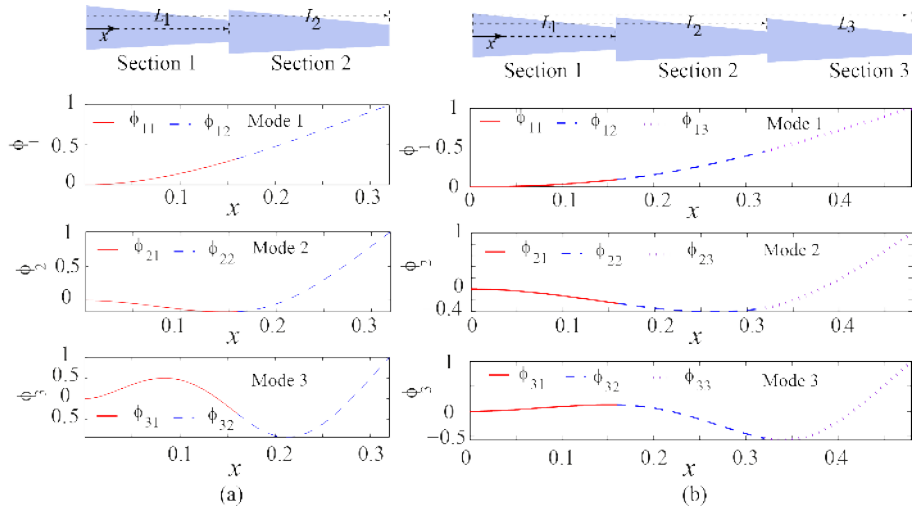

Fig. 6 Analytical mode shapes of bolted cantilever beams with (a) two, and (b) three non-uniform sections.

4.2 Modal Analysis of a Bolted Cantilever Beam with Two Non-Uniform Sections

To analytically compute the mode shapes and frequencies of a bolted beam with two sections, we follow the same approach as discussed above to compute the approximate modeshape of each section. The length of each section is taken as L=0.16 m such that first section ranges from $x = 0$ to $x = L_1 = 0.16$ m and second section ranges from $x = L_1 = 0.16$m to $x = L_2 = 0.32$m. Using the dimensions and properties of the beam, the variation of mass and flexural rigidity for the two sections can be written as,

$$\begin{aligned} m_1(x) &= 0.162 + 0.675x, \quad EI_1(x) = 1.38 + 5.75x. \\ m_2(x) &= 0.054 + 0.675x, \quad EI_2(x) = 0.46 + 5.75x. \end{aligned} \tag{13}$$

To find the frequencies of all the three modes, we first compute the mode shapes using approximate methods in conjunction with the boundary conditions, normalization condition and bolted joint condition, etc., in the following section.

– *First Mode*: The assumed first mode shape ϕ_1 is written in terms of the mode shapes of two sections, i.e., ϕ_{11} and ϕ_{12}, such that $\phi_1 = \phi_{11}+\phi_{12}$. The assumed mode shapes of ϕ_{11} and ϕ_{12} can be written as

$$\begin{aligned} \phi_{11}(x) &= a_0 + a_1\frac{x}{L} + a_2\frac{x^2}{L^2}, \\ \phi_{12}(x) &= b_0 + b_1\frac{x}{L} + b_2\frac{x^2}{L^2} + b_3\frac{x^3}{L^3} + b_4\frac{x^4}{L^4} \end{aligned} \tag{14}$$

where, a_0, a_1, a_2, b_0, b_1, b_2,b_3 and b_4 are unknown coefficients which can be obtained from the boundary conditions, normalization condition, and joint conditions. The equations associated with all the necessary conditions can be written as

$$\begin{aligned} \phi_{11}(0) = 0,\ \phi'_{11}(0) = 0,\ \phi_{11}(L1) = \phi_{12}(L1), \phi'_{11}(L1) = \phi'_{12}(L1), \\ \left(EI(x)\phi''_{11}(x)\right)|_{x=L1} &= -k_{r1}\phi'_{11}(L1) + \left(EI(x)\phi''_{12}(x)\right)|_{x=L1}, \\ \phi_{12}(L2) = 1,\ \phi''_{12}(L2) = 0,\ \phi'''_{12}(L2) = 0, \left(EI(x)\phi'''_{11}(x)\right)|_{x=L1} = \\ \left(EI(x)\phi'''_{12}(x)\right)|_{x=L1}, \end{aligned} \tag{15}$$

where, k_{r1} is the torsional stiffness of the bolted joints located at $x = L1$. Taking $k_{r1} = 0.01$ Nm/rad, the mode shapes of all the sections corresponding to first mode of the bolted beam can be written as

$$\begin{aligned} \phi_{11}(x) &= 16.35x^2 - 22.72x^3, \\ \phi_{12}(x) &= 0.19 - 3.30x + 36.36x^2 - 75.74x^3 + 59.18x^4. \end{aligned} \tag{16}$$

Using the above equation, the modal frequency is found as 14.08 Hz.

– *Second Mode*: To obtain the expression of second mode, we use additional zero position at $x = \alpha = 0.21$ m found from the experiment. Consequently, the order of the assumed polynomial for the second section is increased by one in order to satisfy additional boundary condition, i.e., $\phi_{22}(\alpha) = 0$. Writing the second mode shape as $\phi_2 = \phi_{21} + \phi_{22}$, where, ϕ_{21} and ϕ_{22} are the assumed

mode shapes of two sections which are obtained with $k_{r1} = 0.01$ Nm/rad as

$$\begin{aligned} \phi_{21}(x) &= -23.41x^2 + 106.71x^3, \\ \phi_{22}(x) &= -1.59 + 46.82x - 526.92x^2 + 2581.84x^3 - 5495.401x^4 \\ &\quad +4347.91x^5. \end{aligned} \tag{17}$$

Using Eqs. (3) and (17), we get the second modal frequency as 68.48 Hz. We have also found that the error associated with the zero position $\alpha = 0.21 \pm 0.007$m may vary from $7 - 8\%$.

– *Third Mode*: To obtain the expression of third mode, we use two additional zero locations at $x = \beta = 0.14$m and $x = \alpha = 0.28$ m from the fixed end. Consequently, the order of the assumed mode shape for the first and the second sections are increased by one order each as compared to that in the first mode. Consequently, the assumed mode shapes satisfy additional boundary conditions, i.e., $\phi_{31}(\beta) = 0$ and $\phi_{32}(\alpha) = 0$. Writing the third mode shape as $\phi_3 = \phi_{31} + \phi_{32}$, where, ϕ_{31} and ϕ_{32} are the mode shapes of two sections which are obtained as

$$\begin{aligned} \phi_{31}(x) &= 324.38x^2 - 3474.65x^3 + 8747.44x^4, \\ \phi_{32}(x) &= -30.38 + 750.49x - 6796.61x^2 + 28320.76x^3 \\ &\quad -55315.8x^4 + 41487.75x^5. \end{aligned} \tag{18}$$

Using Eqs. (3) and (18), we get the third modal frequency as 251.33 Hz. The maximum percentage error associated with the variation in measuring zero positions $\beta = 0.14 \pm 0.007$m and $x = \alpha = 0.28 \pm 0.007$ m is found to be less than 2%.

To understand the variation of torsional stiffness k_{r1} on computed frequency, we do sensitivity analysis with respect to different values of k_{r1}. For k_{r1}=0, 0.01, 0.1, 1, 10 Nm/rad, the frequency values of first, second and third modes are mentioned in Table 4. As the stiffness value increases, the first mode fre-

Table 4 Variation of first three modal frequencies of two section bolted beam with bolt parameter k_{r1}.

k_{r1} [Nm/rad]	First Mode [Hz]	Second Mode[Hz]	Third Mode [Hz]
0.0	14.07	68.4808	266.589
0.01	14.08	68.4811	266.598
0.1	14.11	68.4836	266.672
1	14.47	68.508	267.409
10	17.4	68.7326	274.33

Table 5 Frequency comparison for bolted beam with two sections

Mode	Exp. results [Hz]	Anal. results [Hz]	% Error
1st mode	13.1	14.08	7.5
2nd mode	66.5	68.48	3.0
3rd mode	260.25	266.60	2.4

quency is changed by more than 10% only when k_{r1} value increases from 1 to 10. The percentage change in the frequencies of second and third modes are less than 1% and 3%, respectively, when k_{r1} varies from 0 to 10. When we compare the computed values with $k_{r1} = 0.01$ Nm/rad with measured values in Table 5, we get percentage errors of 7.5%, 3.0% and 2.4%. Hence, a smaller value of $k_{r1} = 0.01$ implies that the bolted joint between the two beams provide marginally stiffness to the system of two beams and hence rigidly joined the two beams. For the system of three non-uniform bolted beams, we use $k_{r1} = 0.01$ Nm/rad for both the joints in the following section.

4.3 Modal Analysis of a Bolted Cantilever Beam with Three Non-Uniform Sections

To compute the approximate expression of mode shapes corresponding to first three modes of a bolted cantilever beam with three non-uniform sections as shown in Fig. 6, we define section 1 from $x = 0$ to $x = L_1 = L$, section 2 from $x = L_1 = L$ to $x = L_2 = 2L$, and section 3 from $x = L_2 = 2L$ to $x = L_3 = 3L$. Using the previously defined values of dimensions, the variation of mass, $m(x)$ and flexural

rigidity $EI(x)$ over the three sections can be written as

$$\begin{aligned} m_1(x) &= 0.162 + 0.675x, \quad EI_1(x) = 1.38 + 5.75x. \\ m_2(x) &= 0.054 + 0.675x, \quad EI_2(x) = 0.46 + 5.75x. \\ m_3(x) &= -0.054 + 0.675x, \quad EI_3(x) = -0.46 + 5.75x. \end{aligned} \tag{19}$$

To find the mode shapes of first three modes of bolted beam with three non-uniform sections, we write the combined mode shape in terms of the shape of each section, respectively. Subsequently, we obtain the unknowns associated with the assumed mode shapes by satisfying the boundary conditions, normalization condition and the joint conditions as described for bolted beams with two sections.

– *First Mode*: Writting the first mode shape ϕ_1 in terms of the shapes of all the three sections, i.e., ϕ_{11}, ϕ_{12}, and ϕ_{13}, we get $\phi_1 = \phi_{11} + \phi_{12} + \phi_{13}$. The assumed mode shapes of ϕ_{11}, ϕ_{12}, and ϕ_{13} can be written as

$$\begin{aligned} \phi_{11}(x) = a_0 + a_1\frac{x}{L} + a_2\frac{x^2}{L^2},\ \phi_{12}(x) = b_0 + b_1\frac{x}{L} + b_2\frac{x^2}{L^2}, \\ \phi_{13}(x) = c_0 + c_1\frac{x}{L} + c_2\frac{x^2}{L^2} + c_3\frac{x^3}{L^3} + c_4\frac{x^4}{L^4} \end{aligned} \tag{20}$$

where, a_0, a_1, a_2, b_0, b_1, b_2, c_0, c_1, c_2, c_3 and c_4 are unknown coefficients which can be obtained from the boundary conditions, normalization condition, and joint conditions from the following equations,

$$\begin{aligned} \phi_{11}(0) = 0,\ \phi'_{11}(0) = 0,\ \phi_{11}(L1) = \phi_{12}(L1),\ \phi'_{11}(L1) = \phi'_{12}(L1), \\ \left(EI(x)\phi''_{11}(x)\right)|_{x=L1} = -k_{r1}\phi'_{11}(L1) + \left(EI(x)\phi''_{12}(x)\right)|_{x=L1},\ \phi_{12}(L2) \\ = \phi_{13}(L2),\ \phi'_{12}(L2) = \phi'_{13}(L2), \left(EI(x)\phi''_{12}(x)\right)|_{x=L2} = -k_{r2}\phi'_{12}(L2) \\ + \left(EI(x)\phi''_{13}(x)\right)|_{x=L2},\ \phi_{13}(L4) = 1,\ \phi''_{13}(L4) = 0,\ \phi'''_{13}(L4) = 0, \\ \left(EI(x)\phi'''_{11}(x)\right)|_{x=L1} = \left(EI(x)\phi'''_{12}(x)\right)|_{x=L1}, \\ \left(EI(x)\phi'''_{12}(x)\right)|_{x=L2} = \left(EI(x)\phi'''_{13}(x)\right)|_{x=L2}, \end{aligned} \tag{21}$$

where, k_{r1} and k_{r2} are the torsional stiffness of the bolted joints located at $x = L1$ and $x = L2$. Taking $k_{r1} = k_{r2}$=0.01 Nm/rad, the mode shapes of all the three sections corresponding to first mode of the bolted beam can be written as

$$\phi_{11}(x) = 6.05x^2 - 5.05x^3,\ \phi_{12}(x) = 0.076 - 1.03x + 10.09x^2 - 8.42x^3,$$
$$\phi_{13}(x) = 0.63 - 6.5x + 30.3x^2 - 40.08x^3 + 21.92x^4. \quad (22)$$

The first mode shape is also shown in Fig. 6(b). Using Eqs. (3) and (22), we get the first modal frequency as 6.10 Hz.

– *Second Mode*: Since the second mode shape of the bolted three non-uniform beam has an additional zero position at $x = \alpha = 0.33$ m which is located in third section as shown in Fig. 4(b), the order of polynomial for the third section is increased by one to satisfy the boundary condition, i.e., $\phi_{23}(\alpha) = 0$. Writing the second mode shape as $\phi_2 = \phi_{21} + \phi_{22} + \phi_{23}$, where, ϕ_{21}, ϕ_{22}, and ϕ_{23} are the assumed mode shapes of three sections. Using the same sets of boundary conditions, normalization conditions, condition of additional zero position and joint conditions, we obtain

$$\phi_{21}(x) = -7.16x^2 + 18.92x^3,\ \phi_{22}(x) = -0.02 + 0.56x - 11.94x^2$$
$$+31.54x^3, \phi_{23}(x) = -16.23 + 231.03x - 1279.34x^2 + 3396.03x^3$$
$$-4298.73x^4 + 2108.3x^5. \quad (23)$$

The final second mode shape can also shown in Fig. 6(c). Using Eqs. (3) and (23), we get the second modal frequency as 38.38 Hz. The percentage error in computing frequency due to the variation of zero point $\alpha = 0.33 \pm 0.007$m is found to be less than 5%.

– *Third Mode*: Similarly, the measure mode shape of third mode has two additional zero locations at $x = \beta = 0.23$m and $x = \alpha = 0.37$ m from the fixed end. Consequently, the order of the assumed mode shape for the second section and

the third section are increased by one order each as compared to that in the first mode. Consequently, the assumed mode shapes satisfy additional boundary conditions, i.e., $\phi_{32}(\beta) = 0$ and $\phi_{33}(\alpha) = 0$. Writing the third mode shape as $\phi_3 = \phi_{31} + \phi_{32} + \phi_{33}$, where, ϕ_{31}, ϕ_{32}, and ϕ_{33} are the assumed mode shapes of three sections. The shape of three sections are obtained using the boundary conditions, normalization conditions, condition of additional zero positions and joint conditions with the same values of k_1 and k_2 as

$$\phi_{31}(x) = 5.77x^2 - 23.83x^3,\ \phi_{32}(x) = 0.2 - 5.82x + 64.1x^2 - 266.66x^3 + 354.59x^4, \phi_{33}(x) = -54.50 + 736.71x - 3863.81x^2 + 9796.72x^3 - 12024.83x^4 + 5768.64x^5. \quad (24)$$

The final third mode shape can also shown in Fig. 6(d). Using Eqs. (3) and (24), we get the third modal frequency as 74.98 Hz. The percentage error in computing frequency due to the variation of zero points $\beta = 0.23 \pm 0.007$m and $x = \alpha = 0.37 \pm 0.007$m vary from 1% to 9%.

Finally, when we compare the analytical results with experimental results in Table 6, we find the maximum percentage error of about 14.8%. Error may be due to the approximate mode shapes, minor difference in the symmetry of the tapering and holes provided at the end of the fabricated non-uniform beams, some uncertainties associated with the bolted joints, frequency resolution in the measured signal, etc. It is also found that by increasing the torsional stiffness, we can obtain the changes in the mode shapes and frequencies. Since the values of $k_{r1} = k_{r2} = 0.01$ Nm/rad are found to be small in the present case, therefore, modal frequencies of bolted beams may found to be closer to the monolithic beam with three sections without any bolted joints.

Table 6 Frequency comparison for bolted beam with three sections

Mode	Exp. results [Hz]	Anal. results [Hz]	% Error
1st mode	5.63	6.10	8.35
2nd mode	33.43	38.38	14.8
3rd mode	73.44	74.98	2.0

4.4 Modal Analysis of Three-Sections Monolithic Beam

In this section, we compute modal frequencies of monolithic beam with three sections without any joint by neglecting the terms associated with torsional stiffness at the joints. Using the zero position of second mode at $x = \alpha = 0.36$m and the third mode at $x = \alpha = 0.4$m and $x = \beta = 0.23$m obtained from the experimental mode shapes, we get the final form of the mode shapes using the same procedure as described in the previous section. For the first mode, we get the following shape functions

$$\phi_{11}(x) = 6.05x^2 - 5.04x^3,\ \phi_{12}(x) = 0.08 - 1.03x + 10.08x^2 - 8.40x^3,$$
$$\phi_{13}(x) = 0.63 - 6.48x + 30.25x^2 - 42.02x^3 + 21.89x^4. \quad (25)$$

For the second mode, we obtain the mode shape as

$$\phi_{21}(x) = -10.50x^2 + 24.98x^3,\ \phi_{22}(x) = -0.04 + 0.96x - 17.50x^2 + 41.62x^3,$$
$$\phi_{23}(x) = -20.49 + 291.00x - 1610.05x^2 + 4264.21x^3 - 5389.75x^4 + 2640.77x^5 \quad (26)$$

Similarly, the corresponding mode shapes for the third mode are obtained as,

$$\phi_{31}(x) = 11.56x^2 - 47.53x^3,\ \phi_{32}(x) = 0.33 - 9.82x + 110.99x^2 - 461.40x^3$$
$$+597.17x^4, \phi_{33}(x) = -84.59 + 1137.73x - 5935.53x^2 + 14972.72x^3$$
$$-18312.23x^4 + 8761.62x^5 \quad (27)$$

Using the mode shape expressions, we obtained the modal frequencies from Eq. (3) as 6.10 Hz, 47.54 Hz, and 110.55 Hz corresponding to first three transverse modes.

Table 7 Frequency comparison for three section monolithic beam

Mode	Exp. results [Hz]	Anal. results [Hz]	% Error
1st mode	6.75	6.10	9.63
2nd mode	43.25	47.54	9.9
3rd mode	118.0	110.55	6.74

On comparing the analytical results with the experimental results as mentioned in Table 7, the percentage errors are found to be below 10%. It is also noticed that due to small values of torsional stiffness at the joints and non-trivial mass of bolts, the frequencies of bolted joint are found to be less than that of monolithic beam. Although, the present formulation is useful when the joint acts as a torsional spring especially under free standing structures, it should be modified to include frictional effect to capture more realistic characteristics of bolted joints under different loading conditions. However, the method presented in the paper can be easily extended to the bolted beams of several complicated bolted non-uniform sections where the stiffness of the bolted joint is significant.

5 Conclusions

In this paper, we present theoretical modeling of single non-uniform cantilever beam and bolted cantilever beams with three non-uniform sections to compute the modal frequencies of first three transverse modes. To develop the model, we first carry out experiments to measure the modal frequencies and shapes of single non-uniform cantilever beam with linearly diverging section, bolted beams with two and three sections, monolithic beam with three section, respectively. On comparing the results, we found that the frequencies of bolted beams reduce due to reduction in the stiffness and non-trival mass of bolt at the joints as compared to that of the monolithic beam with three sections without joints. To understand the modeling, we also develop numerical models of cantilever beams with single and three non-uniform sections without joint. On comparing the numerical and experimental results, we found that the model based on the Euler-Bernoulli beams

can be used to develop analytical model. Finally, we develop approximate analytical model to first find the mode shapes using the information of zero position of the experimental mode shapes for the single beam and then compare the results with the experimental and numerical values. Subsequently, we extend the method to model the bolted beams by replacing each bolted joint by a torsional spring of stiffness, $k_r = 0.01$ Nm/rad. On comparing the analytical results with experiment values, we found the maximum percentage error of about 15% is found in the bolted beam with three non-uniform sections. For the case of bolted beam with two sections, the percentage error is found to be less than 10%. The error may be due to the approximate mode shapes as well as differences in the physical dimensions of fabricated non-uniform beams. It is also noticed that experimental, FEA and analytical, all three values match very closely for first mode (less than 10% error), however, difference for higher modes is more (10 – 15%). Finally, we state that the method presented in the paper can be easily extended to the bolted structures with many non-uniform sections.

Acknowledgement

The author thanks Vamsi Krishna for rederiving some formulations and Prashant Kambali for his help in conducting some measurements.

References

1. Tizzi S (2000) Improvement of a numerical procedure for the dynamic analysis of aircraft structures. Journal of Aircraft 37(1): 144-154
2. Platus DH (1992) Aeroelastic stability of slender spinning missiles. AIAA J of Guid Control Dyn 15(1): 144-151
3. Pradhan S, Datta PK (2006) Dynamic instability characteristics of a free-free missile structure under a controlled follower force. Aircr Eng Aerpsp Tec 78(6): 509-514
4. Gupta AK, (1985) Vibration of tapered beams. ASCE J of Struct Eng 111(1): 1936
5. Abrate S, (1995) Vibration of non-uniform rods and beams. J of Sound Vib 185(4): 703-716.

6. Wu J, Ho C (1987) Analysis of wave induced horizontal and torsional coupled vibrations of a ship hull. Aircr Eng Aerpsp Tec 31(4): 235-252
7. Pourtakdoust SH, Assadian N (2004) Investigation of thrust effect on the vibrational characteristics of flexible guided missiles. J of Sound Vib 272(1-2): 287-299.
8. Jaworski JW, Dowell ED (2008) Free vibration of cantilevered beam with multiple steps: comparison of several theoretical methods with experiment. J of Sound Vib 312(4-5): 713-725
9. Zheng DY, Cheung YK, Au FTK and Cheng YS (1998) Vibration of multi-span non-uniform beams under moving loads by using modified beam vibration functions. J of Sound Vib 212(3): 455-467
10. Gaul L, Nitsche R (2001) The role of friction in mechanical joints. Appl Mech Rev 54(2): 93-106
11. Bograd S, Reuss P, Schmidt A, Gaul L, Mayer M (2011) Modeling the dynamics of mechanical joints. Mech Syst and Signal Pr 25(8): 2801-2826
12. Oldfield M, Ouyang H, Mottershead JE (2005) Simplified models of bolted joints under harmonic loading. Comput Struct 84(1-2): 25-33
13. Todd MD, Nichols JM, Nichols CJ, Virgin LN (2004) An assessment of modal property effectiveness in detecting bolted joint degradation: theory and experiment. J of Sound Vib 275(3-5): 1113-1126
14. Ouyang H, Oldfield MJ, Mottershead JE (2006) Experimental and theoretical studies of a bolted joint excited by a torsional dynamic load. Int J of Mech Sci 48(12): 1447-1455
15. Ma X, Bergman L, Vakakis A (2001) identification of bolted joints through laser vibrometry. J of Sound Vib 246(3): 441-460
16. Hartwigsen CJ, Song Y, McFarland DM, Bergman LA, Vakakis AF (2004) Experimental study of non-linear effects in a typical shear lap joint configuration. J of Sound Vib 277(1-2): 327-351
17. Quinn DD (2012) Modal analysis of jointed structures. J of Sound Vib 331(1):81-93
18. Tol Ş, Özgüven H (2004) Dynamic characterization of bolted joints using FRF decoupling and optimization. Mech Syst and Signal Pr 54-55:124-138
19. Chen D-W, Wu J-S (2002) The exact solutions for the natural frequencies and mode shapes of non-uniform beams with multiple spring mass systems. J of Sound Vib 255(2):299-322.
20. Song Y, Hartwigsen CJ, Macfarland DM, Vakakis AF, Bergman LAY (2004) Simulation of dynamics of beam structures with bolted joints using adjusted Iwan beam elements. J of sound vib 273(1-2): 249-276.
21. Eriten M, Kurt M, Luo G, McFarland DM, Bergman LA, Vakakis AF (2013) Nonlinear system identification of frictional effects in a beam with a bolted joint connection. Mech Syst and Signal Pr 39(1-2): 245-264

22. Ahmadian H, Jalali H (2007) Generic element formulation for modelling bolted lap joints. Mech Syst and Signal Pr 21(5):2318-2334
23. S D, Willner K (2015) Investigation of a jointed friction oscillator using the multiharmonic balance method. Mech Syst and Signal Pr 52-53: 73-87
24. Jaumouillá V, Sinou J-J, Petitjean B (2010) An adaptive harmonic balance method for predicting the nonlinear dynamic responses of mechanical systems application to bolted structures. J of Sound Vib 329(19): 4048-4067
25. Ibrahim RA, Pettit CL (2005) Uncertainties and dynamic problems of bolted joints and other fasteners. J of Sound Vib 279(3-5): 857-936
26. Sarkar K, Ganguli R (2013) Closed-form solutions for non-uniform Euler-Bernoulli free-free beams. J of Sound Vib 332(23): 6078-6092
27. Pai PF, Lee S-Y (2003) Non-linear structural dynamics characterization using a scanning laser vibrometer. J of Sound Vib 264(3):657-687
28. Amabili M, Carra S (2012) Experiments and simulations for large-amplitude vibrations of rectangular plates carrying concentrated masses. J of Sound Vib 331(1):155-166